

# Thermostability and Activity Improvements of PETase from *Ideonella sakaiensis*

Jansen Stevenson, Rifqi Zahroh Janatunaim, Aisy Humaira Ratnaputri, Safero Hedi Aldafa, Resmila Rachelisa Rudjito, Dwi Hadi Saputro, Sony Suhandono, Rindia Maharani Putri, Reza Aditama, and Azzania Fibriani\*



Cite This: *ACS Omega* 2025, 10, 6385–6395



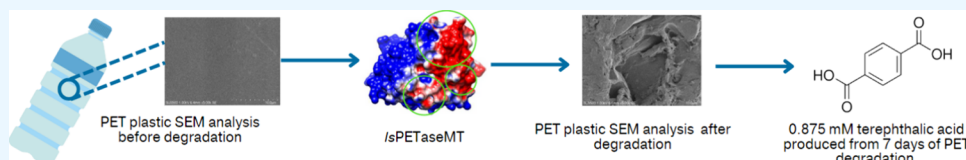
Read Online

ACCESS |

Metrics & More

Article Recommendations

Supporting Information



**ABSTRACT:** Polyethylene terephthalate (PET), a widely used plastic, is a significant environmental pollutant due to its persistence. While the PET-degrading enzyme PETase from *Ideonella sakaiensis* offers promising solutions, its limited activity at higher temperatures hinders its practical application. This study aimed to enhance the PETase performance through protein engineering. We introduced multiple amino acid substitutions to the wild-type *I. sakaiensis* PETase to improve its thermostability, substrate binding, and catalytic activity. Several potential mutant *IsPETases* were generated using computational design and evaluated *in silico*. The selected mutant was then produced in *E. coli* BL21(DE3). Finally, the catalytic activity of the purified mutant *IsPETase* was examined *in vitro* using *p*-nitrophenyl butyrate and PET substrates. *IsPETase<sup>MT</sup>* has been confirmed to be catalytically active and more thermostable with a maximum temperature reaching 60 °C and the *T<sub>m</sub>* value increasing up to 15.3 °C compared to the wild-type PETase, *IsPETase<sup>WT</sup>*. *IsPETase<sup>MT</sup>* also showed better degradation toward the PET plastic film in comparison to *IsPETase<sup>WT</sup>*. Thus, these findings demonstrate successful protein engineering to create a more robust PETase for potential plastic waste management applications.

## 1. INTRODUCTION

Polyethylene terephthalate (PET) is a reversible, reheatable, and easily moldable thermoplastic. As a result, PET is the most widely used thermoplastic polymer resin in the polyester family, with consistently high demand from downstream users annually.<sup>1</sup> The annual production of PET worldwide reached 30.5 million metric tons in 2019, and it is projected to increase to approximately 35.3 million metric tons produced annually by 2024 with continued growth anticipated each subsequent year.<sup>2</sup>

The higher the PET production is, the higher the waste product will be in the environment. The highest waste products were generated from the packaging industry to which PET contributed 33 million metric tons or 27% of total waste in 2015.<sup>1</sup> Meanwhile, its resistance characteristic makes PET difficult to depolymerize and a potential danger to the environment.

Recently, there have been three widely used ways of managing plastic waste: chemically, mechanically, or biologically. PET depolymerization by the chemical process involved a variety of harsh chemicals and expensive costs.<sup>3</sup> Meanwhile, frequently, mechanically recycled PET produced poor-quality products, and the process reduced the quality of material properties.<sup>1</sup> Processing PET waste using thermal

combustion could result in the formation of toxic fumes, which pollute the environment.<sup>3</sup> Alternatively, the biological PET degradation method is environmentally friendly and effective. Biodegradation studies generally use enzymes from microbes, including cutinase, lipase, and esterase.

One of the enzymes that has demonstrated degradation activity toward PET polymers is the leaf-branch compost (LC)-cutinase from *Clostridium thermocellum*, which has an activity to degrade more than 60% of a commercial PET film after 14 days of incubation at 60 °C.<sup>4</sup> However, LC-cutinase has a low binding affinity with PET<sup>5</sup> and needs the addition of calcium ions to increase its melting temperature, which may result in higher costs for industrial applications.<sup>6</sup>

Another available option for PET degradation is the application of PET hydrolase (PETase) and mono-(2-hydroxyethyl)terephthalate hydrolase (MHETase). Synergistically, they completely degrade PET into CO<sub>2</sub> and water.<sup>7</sup> Both

Received: June 4, 2024

Revised: December 16, 2024

Accepted: January 29, 2025

Published: February 12, 2025



of them not only display high activity but are also applicable under mild conditions. Thus, they could be a promising waste management strategy for plastic waste and be applicable on an industrial scale.<sup>8,9</sup>

However, PETase has a heat-labile character and will be inactivated at a temperature above 40 °C.<sup>1</sup> In moderate temperatures around 25–30 °C, PETase could lose its degradation activity after more than 1 day of incubation time. This makes PETase less efficient for industrial applications because PET processing requires a long incubation time as well as a high reaction temperature of around 50–65 °C to enhance the degradation rate. In addition, the long polymer chain surface transition requires a temperature close to the transition temperature in glass ( $T_g = 65$  °C).<sup>10–12</sup>

Some modified PETases have recently been developed to enhance their thermostability, including FAST-PETase ( $T_m = 63.3$ ),<sup>13</sup> HotPETase ( $T_m = 80.5$ ),<sup>13</sup> TurboPETase ( $T_m = 84$ ),<sup>14</sup> and DuraPETase ( $T_m = 52$ ).<sup>15,16</sup> However, since none of them have been applied in the industry yet, intensive research and developments are still needed to provide PETases with improved stability and hydrolysis activity as alternative solutions for PET plastic waste processing.<sup>17</sup>

As previously reported in some studies, introducing several point mutations to *I. sakaiensis* PETase potentially increases its thermostability, while other point mutations improve its affinity to substrates.<sup>18</sup> In this study, we generated a modified PETase by introducing a combination of several point mutations to *I. sakaiensis* PETase to improve not only its thermostability but also its affinity to the substrate. The performances of the modified PETase were predicted through molecular docking and molecular dynamic simulations. Furthermore, we successfully expressed modified PETase in the *E. coli* BL21(DE3) system and evaluated its thermostability and catalytic activity in PET degradation.

## 2. METHODS

**Stability Screening and Mutation Analysis.** The 3D crystal structure of PETase from *Ideonella sakaiensis* was retrieved from the Protein Data Bank (PDB) ([www.pdb.org/pdb](http://www.pdb.org/pdb)) (PDB ID: 6EQE). This model was chosen because of the high resolution (Å ≤ 2) and percentile quality rating that conforms to protein quality standards (blue region).

The stability mutation screening was provided using the FoldX for YASARA software to achieve mutation points that play a role in improving protein stability, as it can also assist in performing protein repair, executing amino acid mutations, and determining Gibbs's free energy ( $\Delta G$ ) values. The three single mutants, which showed the highest value of stability, were combined in the next mutation and called "Stable mutant".

Furthermore, the screening process of the mutants intended for ligand-to-ligand interaction and thermal stability was analyzed in the molecular dynamics step. The three single mutants that had the lowest docking score were combined with the stable mutant to obtain a combined mutant that had high stability and a strong interaction with ligands.

**Molecular Dynamics (MD) Analysis.** MD simulation was performed to evaluate the thermal stability of mutant and wild-type PETase. *IsPETase*<sup>WT</sup> and *IsPETase*<sup>MT</sup> structures were protonated at pH 7 using the PlayMolecule Web server ([www.playmolecule.com](http://www.playmolecule.com)). The system was then solvated with TIP3P water, and Na<sup>+</sup> and Cl<sup>-</sup> were used to neutralize the system. The CHARMM36 force field was applied to the

system.<sup>19</sup> Minimization was done with the steepest descent algorithm and equilibrated with NVT ensemble for 500 ps followed by NPT ensemble for 500 ps with a cutoff 10 Å and a time step of 2 fs. Production dynamics was done at 300, 400, and 450 K. Thermostability was evaluated by rge root mean square deviation (RMSD), root mean square fluctuation (RMSF), and trajectory analysis using VMD 1.9.3.

*IsPETase*<sup>MT</sup> interaction with the substrate was then analyzed with docking simulations. The location of the ligand binding site pocket of the protein was analyzed using the POCASA (Pocket-Cavity Search) 1.1 server. The substrates' 3D conformation was generated using Marvin Sketch 18.28, while the torsion was checked by AutoDock Tools 1.5.6.<sup>20</sup> *IsPETase*<sup>MT</sup>'s interaction with its substrate was investigated through molecular docking using AutoDock Vina.<sup>21</sup> The docking score, expressed as affinity, indicated the strength of this interaction. Visualization using LigPlot, Chimera, and BIOVIA Discovery Studio 2020 revealed hydrophobic interactions and hydrogen bonds between *IsPETase*<sup>MT</sup> and the substrate.<sup>22–24</sup> To further refine the docking score, MMPBSA simulation was conducted at 300 K, employing the same molecular dynamics (MD) protocol. Gibbs free energy of binding between the substrates and the PETase mutant was then calculated using 500 frames from the MD simulation.

**Potential Electrostatic Visualization.** The effect of mutations on the protein surface characteristics was analyzed by comparing the electrostatic potential of mutants to the wild type using the APBS method. The APBS calculations were performed using the AutoDock Tools version 1.5.6 software. Subsequently, the data were visualized in three dimensions using Chimera.

**Expression of PETase.** The optimized codon wild-type and mutant PETase genes were synthesized<sup>23</sup> and subcloned into the pET-22b(+) vector between *Bam*H I and *Hind*III restriction sites by GenScript. Before expression, colonies were confirmed through colony PCR, plasmid isolation, and DNA sequencing. The optimum expression conditions of recombinant protein were determined using varying concentrations of IPTG (0, 0.25, 0.5, and 1 mM), temperatures (24 and 37 °C), and induction durations (8, 16, and 24 h). The recombinant protein expression subsequently was analyzed using the SDS-PAGE method (Bio-Rad), and the bands formed on the gel were further analyzed using ImageJ to determine the percentage of protein concentration.

**Enzyme Purification and Confirmation.** The purification system was carried out using a Ni-NTA affinity chromatography column (Thermo Fisher). The expression supernatant (concentrated 20×) was added with an equilibration buffer (1:1) to the purification column. Subsequently, samples were dialyzed against PBS using Amicon Ultra-15 10 kDa at 4 °C. The purified enzymes were used in SDS-PAGE, Western blot, and catalytic assay.

To confirm the presence of the protein, a Western blot analysis was conducted. Initially, the purified PETase ( $\pm 0.5$  mg/mL) was transferred onto a PVDF membrane (Thermo Fisher Scientific) using the eBlot L1 Protein Transfer System (GenScript Inc.). The blots were then blocked with 1% skim milk in TBS-T (pH 7.2). Detection involved the use of anti-His tag mouse IgG and horseradish peroxidase (HRP)-conjugated goat antimouse IgG. The Western blot analysis was carried out using a colorimetric method with luminol (LI-

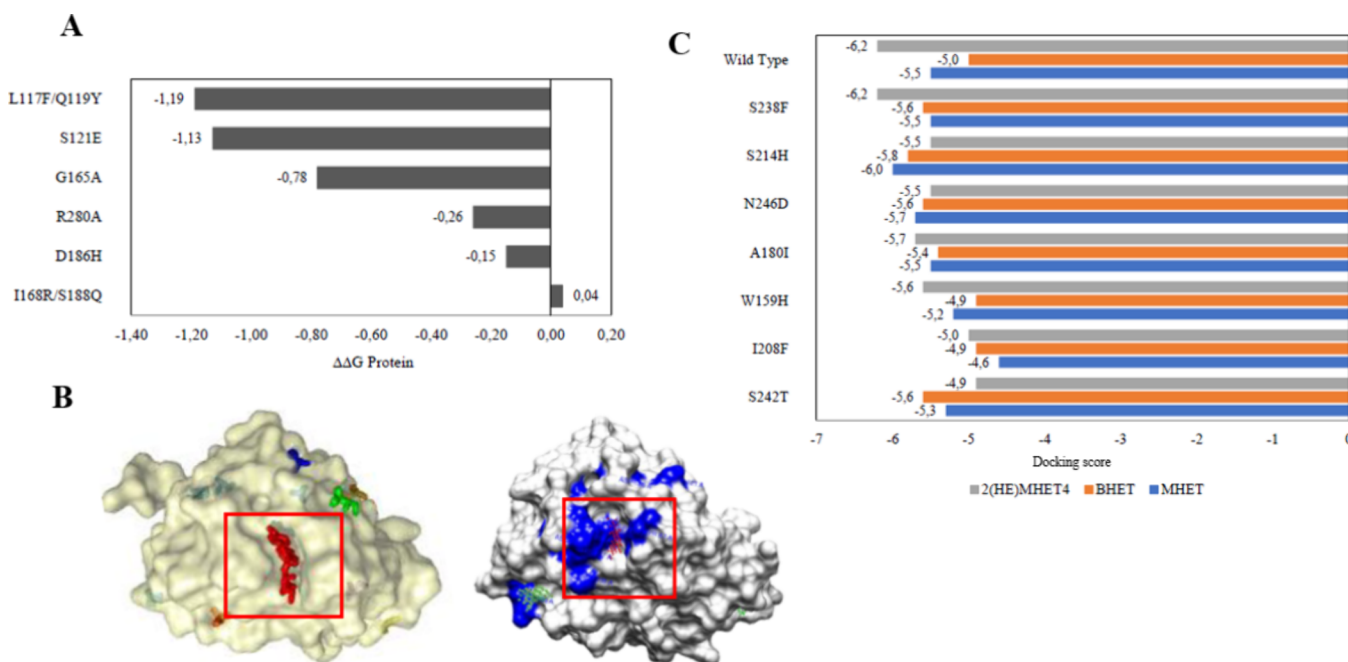


**Figure 1.** Stability, molecular docking, and electrostatic potential study of the mutant PETase. (A) Free energy score of a single mutation in kcal/mol. A score less than  $-0.5$  shows the stability of the protein. (B) Ligand binding pockets on PETase based on web servers PDBSum and POCASA 1. (C) Sequence of docking values of PETase single mutants to three major ligands, namely, 2(HE)MHET4, MHET, and BHET.

COR), and the results were read using the C-Digit Blot Scanner (LI-COR).

**Catalytic and Thermostability Assay.** The catalytic and thermostability assays for PETase were conducted using *p*-nitrophenyl butyrate (Sigma-Aldrich) and SYPRO Orange dye (Sigma-Aldrich). For these assays, 1 mM *p*-nitrophenyl butyrate in 50 mM phosphate buffer (pH 7.2) was utilized to test the activity and thermostability of PETase. Each sample was incubated for 10 min at 24 (room temperature), 30, 40, 50, 60, and 70 °C. The release of *p*-nitrophenol (pNP) was monitored at 415 nm using a GloMax Microplate Reader (Promega). Purified PETase diluted in PBS served as the negative control. The concentration of the purified protein was first determined using a NanoDrop UV/vis Spectrophotometer (Thermo Fisher Scientific).

Thermostability analysis of PETase was performed to determine the melting temperatures ( $T_m$ 's) using differential scanning fluorimetry (DSF). Purified PETase of 47.5 μL (0.5 mg/mL, in PBS solution, pH 7.4) was prepared, and 2.5 μL of 50× SYPRO orange solution in ddH<sub>2</sub>O was added to the final volume of 50 μL. DSF studies were carried out using a Biorad CFX96 real-time PCR system set on the FRET channel using 490 nm excitation and 580 nm emission filters. Samples were heated from 25 to 95 °C at 0.05 °C/s. The  $T_m$  value was determined from the first derivatives of the melting curve in the CFX Manager Software (Biorad).

**Hydrolysis Activity of PETase on PET Film.** The hydrolysis activity of PETase was assessed using a PET film (Goodfellow, ES301460), which was cut into 5 mm diameter circles. The films were sequentially washed with 1% SDS (w/v), ethanol, and distilled water for 30 min each followed by air drying. Subsequently, the PET film was incubated with 70 μL of purified enzyme solution in 430 μL of buffer (50 mM Na<sub>2</sub>CO<sub>3</sub>-NaHCO<sub>3</sub>, pH 9.0) for 168 h at 40 °C. Post-incubation, the films were washed, air-dried, and then analyzed using scanning electron microscopy (Hitachi SU3500).

Afterward, the remaining enzyme and buffer solution were analyzed using HPLC (Shimadzu 20A) with a column size of 5 μm, 4.6 × 150 mm. The mobile phases used were deionized water (A), methanol (B), and 1% acetic acid (C). The flow rate was set at 1 mL/min, and terephthalic acid was detected at a wavelength of 240 nm.<sup>25</sup>

### 3. RESULTS AND DISCUSSION

**3.1. Single Mutation of the Recombinant *Is*PETase.** PETase amino acid mutations were carried out in stages, starting with a single mutation in each protein followed by a combination of mutations from single mutants that exhibited the best stability values. Prior to introduction of mutation using FoldX, improvements were made to the *Is*PETase model (PDB ID: 6EQE) to correct poor torsion angles, conflicting van der Waals bonds, and total energy discrepancies, ensuring a low  $\Delta G$  value that indicates stabilization. An increase in stability from a  $\Delta G$  of 41.14 to  $-24.37$  kcal/mol ( $\Delta\Delta G$  of  $-65.51$  kcal/mol) was observed after improvements of the protein model.

In this study, residues L117 and Q119 were mutated in combination because they can form a  $\pi-\pi$  “T-shaped” interaction with Tyr87, a residue that forms an oxyanion hole.<sup>25</sup> An oxyanion hole is a pocket structure on the active site of the enzyme that aids in binding to oxyanions (oxygen-containing anions), thus stabilizing the transition state in protein–ligand binding.<sup>26</sup> Similarly, mutations I168R and S188Q were introduced simultaneously because the guanidine group on R168 can form new hydrogen bonds with the amide oxygen and oxygen atoms of Q188. Additionally, the I168R amino acid change results in the formation of a new salt bridge with residue D186,<sup>26</sup> as confirmed by supporting analyses using the CIB and ESBRI web servers that showed the addition of four hydrogen bonds and six salt bridges in the mutant *Is*PETase.

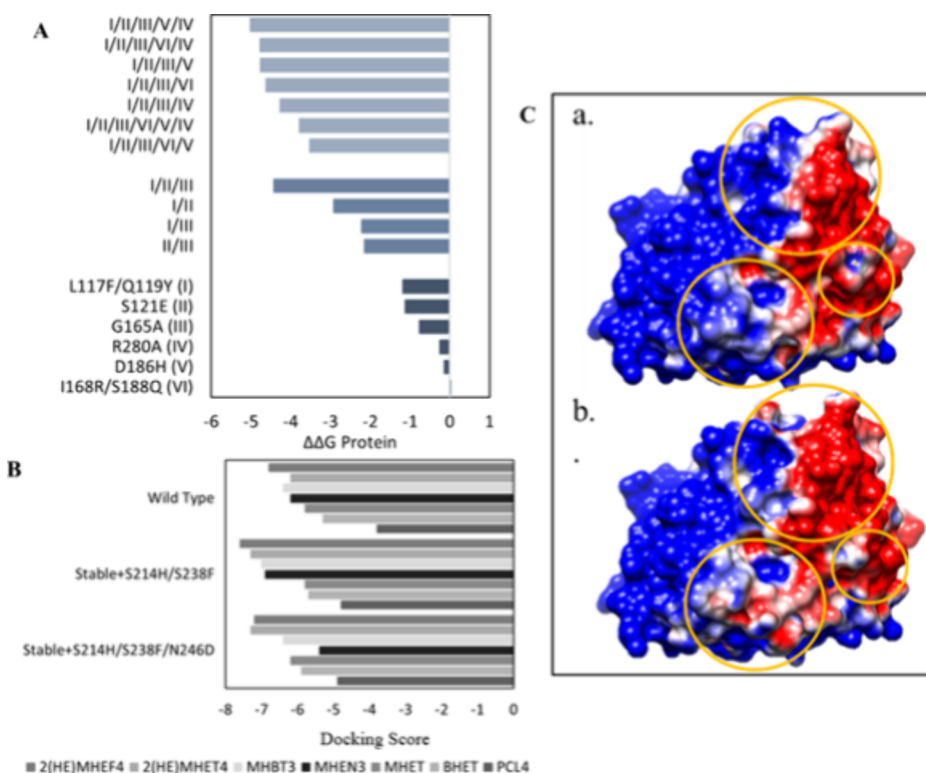


**Figure 2.** Stability, molecular docking, and electrostatic potential study of the mutant PETase. (A) Free energy score of single and combination mutations in kcal/mol. A score less than  $-0.5$  shows the stability of the protein. (B) Binding energies of ligands docked against PETase combination mutants were between the most stable mutant in A and the strongest affinity mutant in B. (C) Visualization of the mutation effect to the potential electrostatic surface of PETase: (a) *IsPETase*<sup>WT</sup> and (b) *IsPETase*<sup>MT</sup>.

Four mutants were identified to increase the stability of *IsPETase*: L117F/Q119Y, S121E, and G165A, while the other three mutants have a neutral effect on the protein (Figure 1A). The presence of L117F and Q119Y mutants, which have the highest level of stability, indicates that the stability of the oxyanion hole region can significantly affect the overall protein stability. This is beneficial for the enzyme because these mutants can synergize to enhance both stability and interaction with ligands. The S121E mutation increases protein stability through a water-mediated hydrogen bond formed by the glutamine residue with the N172 residue. Meanwhile, the G165A mutation reduces the conformational entropy of the locally unfolded protein.<sup>18,26</sup>

In molecular docking studies, identifying the location of the binding pocket is crucial for accurately placing the ligand in the desired area and also serves as a parameter for creating grid boxes in AutoDock. Binding pocket analysis can be performed using data from PDBSum included in the data model or additional web servers, such as POCASA 1.1. Based on the analysis using PDBSum and POCASA, it was found that both tools identified the same binding area. The largest area displayed in POCASA 1.1 with Rank 1 (Pocket 19) corresponds to Cluster 1 in PDBSum, where the most ligand attachment occurs and where catalytic triads and residues that interact with ligands are located (Figure 1B). The red box highlights the ligand binding pocket area on PETase.

Molecular docking studies were conducted between single mutants obtained from references and three main ligands for PETase: 2(HE)MHET4 (a mimic of PET polymer), BHET, and MHET.<sup>25,26</sup> By comparing the molecular docking results of mutant *IsPETases* with the wild type, the results revealed

that the S238F mutant exhibited the highest affinity for 2(HE)MHET4 at  $-6.2$  kcal/mol followed by S214H that showed a high affinity for BHET at  $-5.8$  kcal/mol and N246D with the highest affinity for MHET at  $-5.7$  kcal/mol (Figure 1C). Even though their levels were not significantly higher, the mutant PETases demonstrated better binding abilities with substrates than the wild type.

The S238F mutant enhances the interaction with the ligand through its aromatic side chain, facilitating easier interaction with the ligand. In the S214H mutation, the substitution of serine with histidine improves the aromatic-tunnel shape, thereby increasing the enzyme's ability to bind ligands. This increase in the aromatic side enhances hydrophobic interactions on the surface and within the protein.<sup>18,27</sup> Meanwhile, the N246D mutation, located near the ligand-binding site, primarily contributes to the formation of new salt bridges with R280 rather than hydrophobic or hydrogen interactions with the ligands.<sup>18,27</sup> To further investigate the role of the N246D mutant in binding various substrates, additional analysis was performed, focusing on its combination with other mutants. This will be elaborated on in the following section.

**3.2. Multiple Mutations of the Recombinant *IsPETase*.** After a single mutation was conducted, four individual mutations of PETase were identified for enhancing protein stability, specifically, L117F/Q119Y, S121E, and G165A, while the others gave neutral effects on the protein (Figure 2A, Table S1). Subsequently, these four mutants were combined with other neutral mutants.

The introduction of a mutation on D186H and R280A increased the stability by up to  $-5.0$  kcal/mol, indicating the

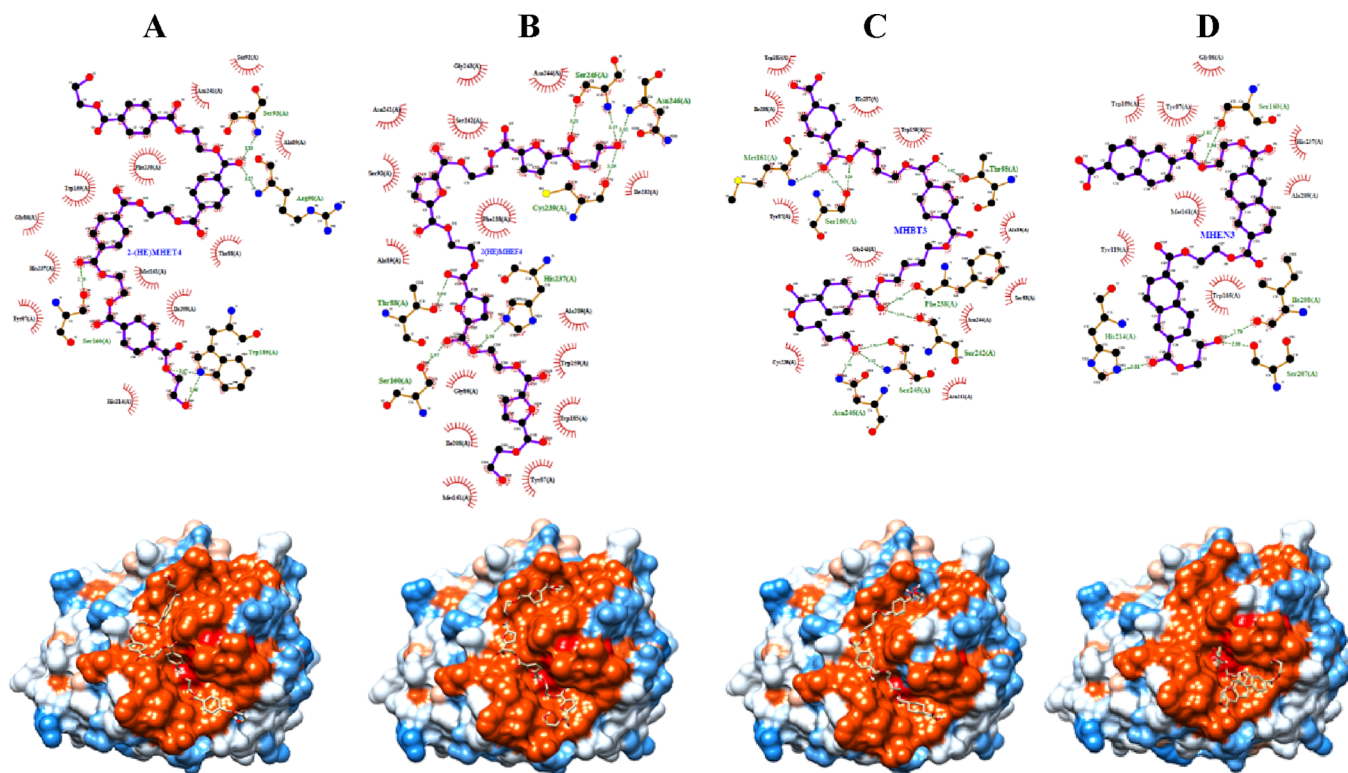


**Figure 3.** Visualization of 2D amino acid residue interaction by LigPlot<sup>+</sup> (top) and the 3D binding ligand in the pocket by Chimera (bottom) in *IsPETase*<sup>MT</sup> against (A) 2-HE(MHET)<sub>4</sub>, (B) 2-HE(MHEF)<sub>4</sub>, (C) MHBT<sub>3</sub>, and (D) MHEN<sub>3</sub> ligands.

stabilization of *IsPETase*. This stabilized combination was labeled as a “stable mutant”. Combining stable mutants with those exhibiting the highest affinity (S214H, S238F, and N246D) demonstrated that pairing mutants S214H and S238F within a stable mutant resulted in a lower energy value compared to combining all three highest affinity mutants separately, yielding  $-7.38$  and  $-7.26$  kcal/mol, respectively (Figure 2B). These outcomes may be attributed to the potential incompatibility between the mutant interaction of R280A and N246D, where alanine possesses a hydrophobic residue, while aspartate carries a negative residual charge.<sup>8</sup>

Furthermore, we designed the highest affinity and most stable recombinant PETase with eight mutation sites PETase<sup>L117F/Q119Y/S121E/G165A/D186H/R280A/S214H/S238F</sup> as *IsPETase*<sup>MT</sup>. An *in silico* model has been built to predict the 3D structure of PETase with multiple mutations (Figure 2C, Table S1). Each of the mutations has a role in improving the PETase activity and temperature stability. The residues of L117 and Q119 can form a “T-shaped”  $\pi$ – $\pi$  interaction with Tyr87 (residues that form oxyanion holes)<sup>18</sup> and trigger the stabilization of the transition state in protein–ligand binding.<sup>26</sup> The mutation of aspartate to histidine in D186H assisted in the formation of water-mediated hydrogen bonds in S121E and Asn172. In addition, negative charges in aspartate could cause polarity collisions between high negative charges; thus, mutation to histidine, which had a slightly positive charge, could stabilize the area.<sup>8</sup> Moreover, the mutation of arginine to alanine in R280A changed the surface of the protein,<sup>26</sup> especially in the loop, which may be able to increase protein stability.

**3.3. Interaction of *IsPETase*<sup>MT</sup> with Substrates.** The molecular docking analysis showed that the *IsPETase*<sup>MT</sup> had a stronger affinity for the monomer of PET with a docking value

of  $-7.3$  kcal/mol compared to the *IsPETase*<sup>WT</sup> value of  $-6.2$  kcal/mol. *IsPETase*<sup>MT</sup> was also able to interact with the other polyesters 2-HE(MHEF)<sub>4</sub> and MHBT<sub>3</sub> (Figure 3B,C, Table S2). In addition, the *IsPETase*<sup>MT</sup> also had better affinity than the *IsPETase*<sup>WT</sup> to MHEN<sub>3</sub> and PCl<sub>4</sub> (Table S2). Meanwhile, in MHET and BHET, mutant affinity was not significantly different from the wild type (Table S2).

In the analysis of hydrophobic interactions and hydrogen bonds, the similarity of interactions with references<sup>17,26–30</sup> between the main ligand 2-HE (MHET)<sub>4</sub> and the wild type was better than the *IsPETase*<sup>MT</sup>, with the results of respective interactions being 63.6 and 45.5%. The polyester ligand that interacted strongly with the *IsPETase*<sup>MT</sup> was MHBT<sub>3</sub> with a total interaction of 54.5%. Meanwhile, the docking simulation results showed that *IsPETase*<sup>MT</sup> and *IsPETase*<sup>W</sup> have similarity of interactions with 2-HE(MHEF)<sub>4</sub>.

The 3D visualization of *IsPETase*<sup>MT</sup> showed that the ligands 2-HE(MHET)<sub>4</sub>, 2-HE(MHEF)<sub>4</sub>, and MHBT<sub>3</sub> bound to the pocket and aromatic tunnel area of PETase (Figure 4). The visualization of the PETase surface showed that there was a change in the charge around the binding pocket after mutation (Figure 2D). After being mutated, the electrostatic potential of the binding site on the PETase protein becomes more neutral (hydrophobic) or negative than the wild type. It makes the polyester ligands easy to attach to the area; thus, the affinity was stronger, and the interaction was wider.

The Gibbs free energy values between *IsPETase*<sup>WT</sup> and *IsPETase*<sup>MT</sup> in the presence of substrates were determined by using the MMPBSA method. The comparison of  $\Delta G$  PETase with the BHET and 2MHET substrates is depicted in Figure 4. The Gibbs free energy binding values for the *IsPETase*<sup>WT</sup>-BHET and *IsPETase*<sup>WT</sup>-2MHET complexes are  $-16.41$  and  $-18.75$  kJ/mol, respectively. Following combined mutations,

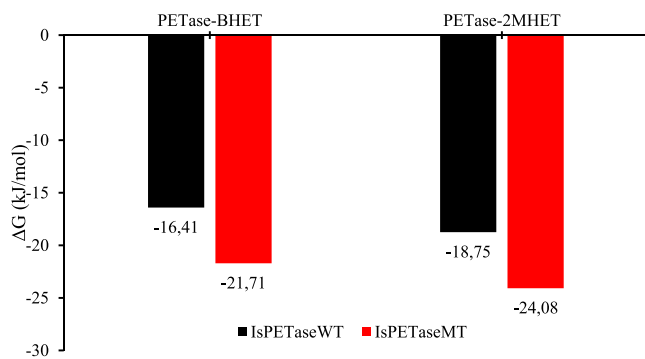


**Figure 4.** Gibbs free energy binding of *IsPETase*<sup>WT</sup> and *IsPETase*<sup>MT</sup> to the BHET and 2MHET substrates that resulted from MMPBSA simulation.

more negative  $\Delta G$  values were obtained, resulting in *IsPETase*<sup>MT</sup>-BHET and *IsPETase*<sup>MT</sup>-2MHET complexes with  $\Delta G$  binding values of  $-21.71$  and  $-24.08$  kJ/mol, respectively. These findings suggest that *IsPETase*<sup>MT</sup> exhibits a stronger binding affinity compared to *IsPETase*<sup>WT</sup> for BHET and 2MHET ligands, with  $\Delta\Delta G$  values of  $-5.30$  and  $-5.33$  kJ/mol, respectively.

**3.4. Thermostability Assessment with MD Simulation.** The results of MD simulation demonstrate that *IsPETase*<sup>MT</sup> exhibits superior thermal stability compared to

*IsPETase*<sup>WT</sup> (Figure 5). *IsPETase*<sup>MT</sup> gives a lower RMSD in comparison to *IsPETase*<sup>WT</sup>, suggesting that the mutation results in fewer structural conformational changes during the simulation when compared to the wild type. From the 300 K MD simulation results, it can be observed that RMSD fluctuations reach up to  $2.0 \text{ \AA}$  for *IsPETase*<sup>WT</sup>, while *IsPETase*<sup>MT</sup> fluctuates only around  $1.3 \text{ \AA}$ .

To assess their stability at high temperatures, the MD simulation temperature was increased to 450 K to accelerate the structural change observation. At a time simulation of 30 ns, the RMSD of *IsPETase*<sup>WT</sup> exceeds  $6 \text{ \AA}$ , while *IsPETase*<sup>MT</sup> remains stable around  $6 \text{ \AA}$ . The trajectory analysis aligns with the RMSD analysis, clearly indicating that *IsPETase*<sup>MT</sup> preserves its structural integrity for a duration of 60 ns, while structural damage in *IsPETase*<sup>WT</sup> begins at 30 ns (Figure 5). Our results suggest that the mutation enhances the thermal stabilization of PETase.

To evaluate mutations that are crucial for maintaining the structural stability of *IsPETase*<sup>MT</sup>, RMSF analysis was conducted (Figure 6). Based on the RMSF analysis, almost all mutation points were revealed to play a role in decreasing RMSF value during a 100 ns simulation. The cumulative effect of mutations applied to PETase can diminish structural flexibility, imparting greater rigidity and, in turn, boosting the thermal stability of PETase.

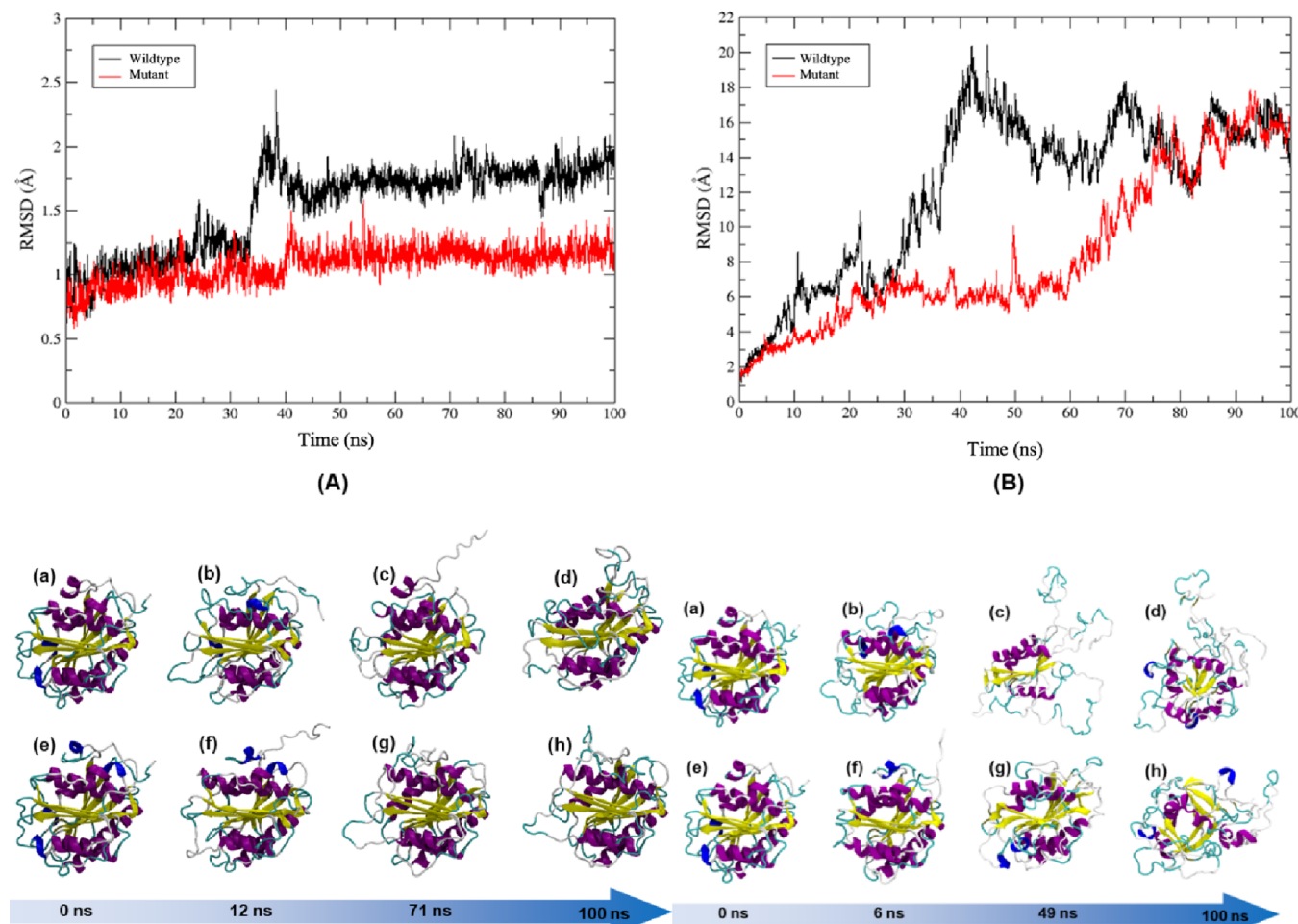


**Figure 5.** Structural evolution of *IsPETase*<sup>WT</sup> (a–d) and *IsPETase*<sup>MT</sup> (e–h) during 100 ns simulation at 450 K.

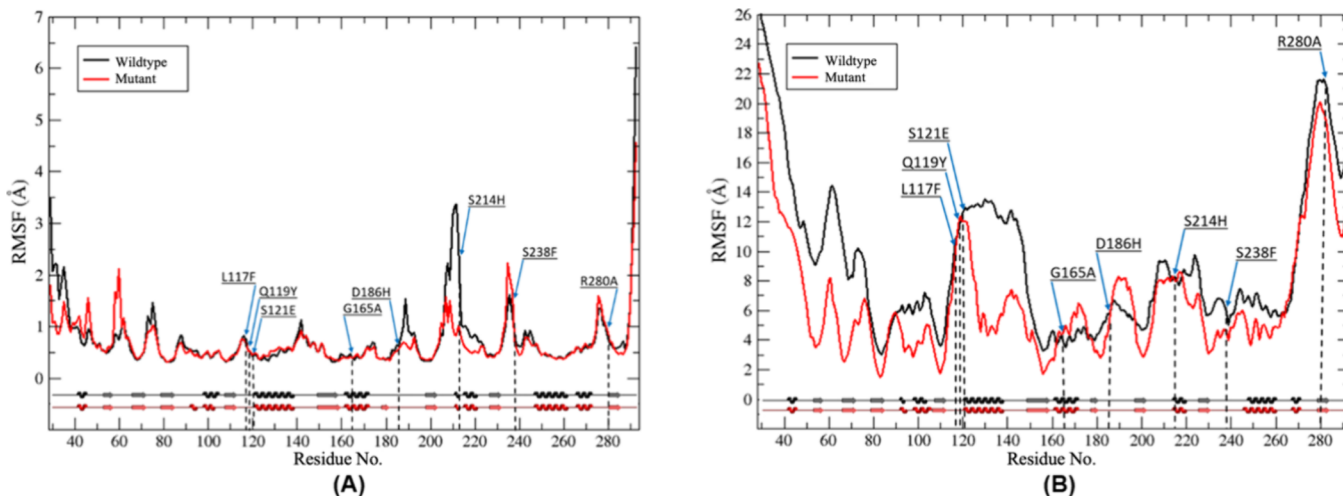


**Figure 6.** RMSF profile of *IsPETase*<sup>WT</sup> and *IsPETase*<sup>MT</sup> at (A) 300 K and (B) 450 K.

**3.5. Production of PETase.** The *IsPETase*<sup>WT</sup> and *IsPETase*<sup>MT</sup> were confirmed to be present in the extracellular fraction in the ~30 kDa band. This was supported in nontransformant *E. coli* where no band was detected in the same region as transformant *E. coli* (Figure 7). In the *IsPETase*<sup>WT</sup>, an additional band of ~30 kDa was identified, indicating the presence of PETase.<sup>31</sup> From the SDS-PAGE results, it was found that *IsPETase*<sup>WT</sup> and *IsPETase*<sup>MT</sup> can be expressed and secreted in *E. coli* in the extracellular fraction using the Sec-dependent signal peptide pelB (Figure 7). The results of SDS-PAGE and ImageJ analysis showed that the optimum PETase production was obtained at 24 °C for 24 h and with an IPTG concentration of 0.25 mM.

**3.6. PETase Catalytic and Thermostability Profile.** The catalytic activity of both PETases was measured in the temperature range of 24–60 °C using pNPB as a substrate. The activity of *IsPETase*<sup>WT</sup> was maximum at 30 °C and stable only at temperatures ranging from 30 to 40 °C. Then, *IsPETase*<sup>WT</sup> activity decreased rapidly at 50 °C and started to be inactive at 60 °C. Meanwhile, in the *IsPETase*<sup>MT</sup>, the activity increased gradually from 20 to 60 °C, reached a maximum activity at 60 °C, and still had activity up to 70 °C (Figure 8A). There are also similar results in the *IsPETase*<sup>TMK95N/F201I</sup> mutant that has thermostability reaching 60 °C but lower activity at low temperatures.<sup>26</sup> Other studies that showed similar results were the DuraPETase<sup>S214H-I168R-W159H-S188Q-R280A-A180I-G165A-Q119Y-L117F-T140D</sup> that withstood the thermostability test for 3 days of incubation in 60 °C temperature.<sup>25</sup> Related to the result, we observed the thermostability profile of PETases by determining the melting temperature value ( $T_m$ ) using the differential scanning fluorimetry (DSF) method. The  $T_m$  value of *IsPETase*<sup>WT</sup> is 40.3 °C, whereas that of *IsPETase*<sup>MT</sup> increased by 15.7 to 66 °C (Figure 8B).

Each mutated residue played an important role in increasing thermostability and affinity toward ligands. A previous study reported other mutations at L117F and Q119Y that played a role in improving the packaging of the protein surface and interior to be more hydrophobic and increasing the melting temperature ( $T_m$ ) of the protein. This indicates an increase in protein thermal stability.<sup>25,26,32</sup> Besides, the mutation at S214H, S238F, and G165A was used to maintain conformation and protein folding to make the mutated protein more

stable.<sup>25,26,33,34</sup> The mutation at S121E and R280A also proved to make the mutated protein more thermostable as was shown in reports regarding FAST-PETase, which has the combination of mutation at both sites as well as R224Q and N233 K and reached a maximum activity toward PET film at 50 °C.<sup>33</sup> Similar results were also obtained in *IsPETase*<sup>S121E/D186H/R280A</sup>, with the  $T_m$  value increased by 8.81 °C and activity detected to be up to 14-fold higher at 40 °C in comparison to the wild type.<sup>35</sup> The point mutation found in *IsPETase*<sup>S121E/D186H/R280A</sup> is also utilized as a template for the directed evolution of IsPETase, resulting in the generation of HOT-PETase through successive rounds of saturation mutagenesis employing NNK codons. The engineered HOT-PETase was detected to maintain optimal activity up to 80 °C, near the PET polymer glass transition temperature, hence optimizing the PET degradation process.<sup>36</sup> Unfortunately, since our research did not include a directed evolution process, the *IsPETase*<sup>MT</sup> that was produced only shows remarkable thermostability up to 60 °C as shown in Figure 8.

**3.7. PET Film Hydrolysis.** The observation was continued by analyzing the PETase hydrolytic activity using a PET film (from the supplier GoodFellow) as a substrate. Before testing, the PETase concentration was equalized to 0.5 mg/mL. Although the optimal activity temperature of *IsPETase*<sup>MT</sup> is 60 °C, the observation was carried out at 40 °C to standardize the treatment with *IsPETase*<sup>WT</sup>, which only has degradation activity up to 40 °C. This standardized treatment allows for a comparison of the degradation results on PET. The PET plastic was damaged compared with the control (Figure 9). The *IsPETase*<sup>WT</sup> seemed to erode and form spiderweb-like pores on the PET film. The hydrolysis activity of *IsPETase*<sup>MT</sup> appears to be successfully improved. From the visual results, it could be seen that the damage caused by *IsPETase*<sup>MT</sup> appears to be greater in degrading the coating on the surface of PET plastic film compared to *IsPETase*<sup>WT</sup>. Several amino acid residue mutations played a role in improving the catalytic activity of PETase. Mutating R280A could make PETase more hydrophobic and form a nonprotruding cleft so that it can make PET substrate binding more stable.<sup>24</sup> The mutation at S214H could also increase the aromaticity in the binding pocket as well as increase the activity toward PET substrates.<sup>29</sup> Furthermore, similar results were also found in the S238F/W159H double mutant PETase where S238F can change the

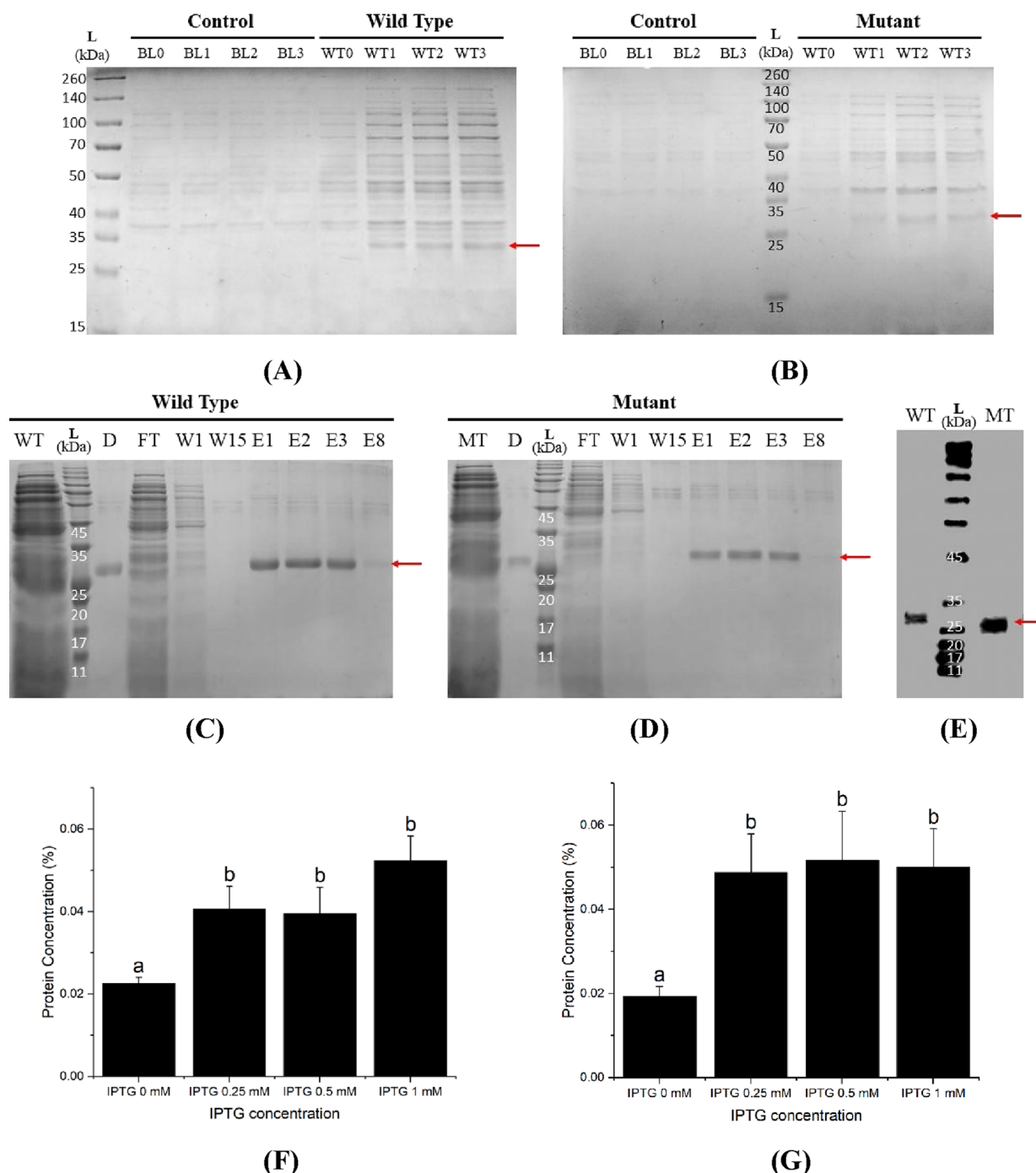


**Figure 7.** Visualization of expressed (A) *IsPETase*<sup>WT</sup> and (B) *IsPETase*<sup>MT</sup> using SDS-PAGE shows ~30 kDa sized band. Visualized purified (C) *IsPETase*<sup>WT</sup> and (D) *IsPETase*<sup>MT</sup> using the Ni-NTA purification system and SDS-PAGE. (E) Visualized Western blot PETase using chemiluminescence as an immunodetection system (L: protein ladder; WT: *IsPETase*<sup>WT</sup>; MT: *IsPETase*<sup>MT</sup>; D: dialysis; FT: flow-through; W: wash; and E: elution). A red arrow points to bands at approximately 30 kDa, which indicate the presence of PETase. The graphic shown is the result of ImageJ analysis for calculating the protein concentration ratio of the (F) *IsPETase*<sup>WT</sup> and (G) *IsPETase*<sup>MT</sup> band to the total protein concentration. The optimal concentration of IPTG used to induce optimum PETase protein fusion production is 0.25 mM.

binding cleft that was an integral part of the aromatic interaction to increase the binding activity on PET substrates.<sup>32,37</sup>

The results indicate that both *IsPETase*<sup>WT</sup> and *IsPETase*<sup>MT</sup> enzymes exhibit degradation activity against the PET film, with the most significant damage observed from the incubation with the *IsPETase*<sup>MT</sup>. Therefore, further analysis to quantify the yield of terephthalic acid (TPA) was done only for

*IsPETase*<sup>MT</sup>. TPA yielded from the degradation of the PET film by *IsPETase*<sup>MT</sup> was quantified using HPLC after 3 min of retention time. After 7 days of incubation with *IsPETase*<sup>MT</sup>, the TPA concentration obtained was 0.875 mM (Figure S4). While this result demonstrates significant and specific degradation activity between the enzyme and the PET substrate, a study conducted by Menzel et al. reported that incubation of *IsPETase*<sup>WT</sup> with PET substrate for 4 days

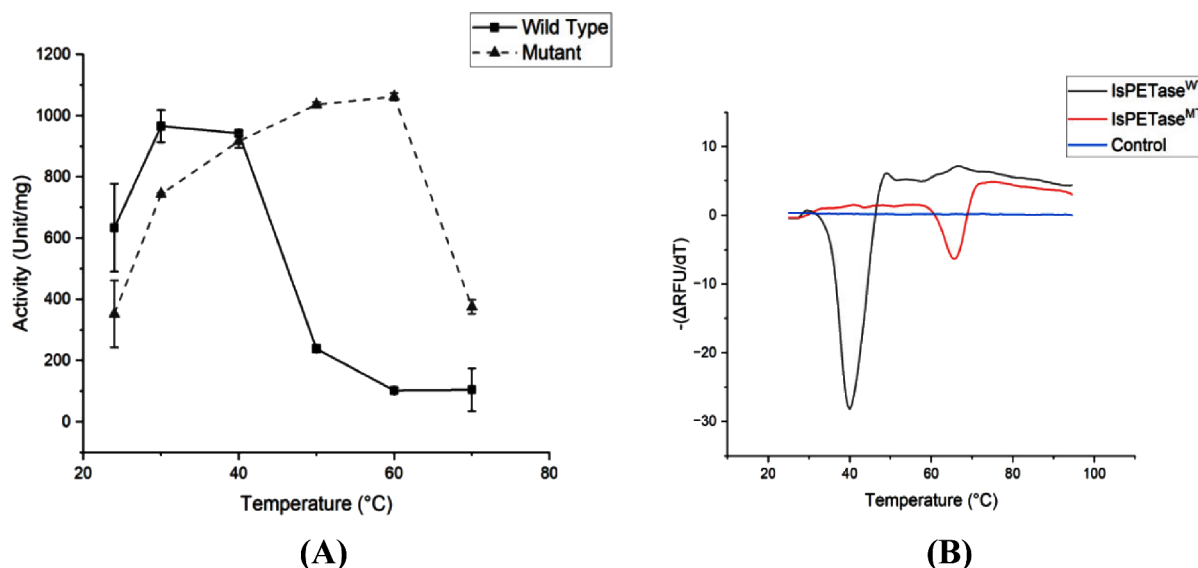


**Figure 8.** Characteristics of PETase (A) activity profile determined using p-NPB as protein substrate in various temperatures ranging from 24 to 60 °C. *IsPETase*<sup>WT</sup> shows the maximum activity as well as thermostability at a temperature ranging from 30 to 40 °C, and its activity decreases rapidly when the temperature goes higher than 40 °C. In comparison, *IsPETase*<sup>MT</sup> shows increasing activity and thermostability at a temperature ranging from 20 to 60 °C, with maximum activity as well as thermostability demonstrated at 60 °C. (B) Thermostability profile defined in melting temperature ( $T_m$ ) curves of PETase using the DSF method. *IsPETase*<sup>WT</sup> has a  $T_m$  value of  $40.3 \pm 0.5$  °C, and *IsPETase*<sup>MT</sup> has a  $T_m$  value  $66 \pm 0.4$  °C.

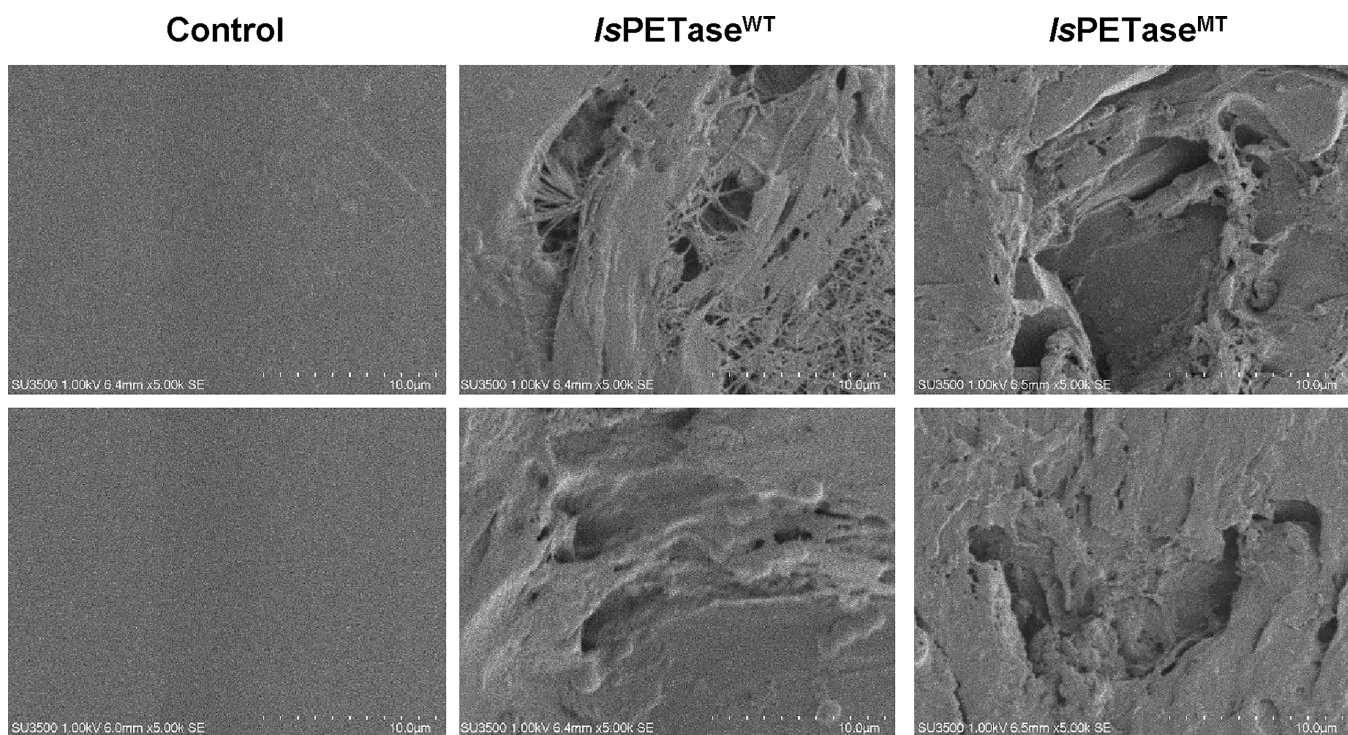


**Figure 9.** Visualized SEM analysis in the PET film treated by secreted PETase at 40 °C for 168 h for the control PET film in buffer solution (A, D), *IsPETase*<sup>WT</sup> (B, E), and *IsPETase*<sup>MT</sup> (C, F). The PET film treated using *IsPETase*<sup>MT</sup> has greater damage than *IsPETase*<sup>WT</sup>.

produced 1.3 mM of terephthalic acid.<sup>38</sup> The main two factors that are possibly contributing to the lower production of TPA compared to *IsPETase*<sup>WT</sup> are the formation of aggregates and/or enzyme denaturation, especially after a long incubation period.<sup>39</sup> This assumption was confirmed by a report from Wei et al.<sup>40</sup> that *IsPETase* tends to lose its activity after 1 h at temperatures near or above 40 °C. Unlike other PET hydrolytic enzymes, LCC can maintain its degradation activity

toward commercial PET bottles and its thermostability for up to 3 days at 65 °C. However, the LCC that was used can maintain its activity and thermostability with the addition of calcium ions using 35 mM CaCl<sub>2</sub>.<sup>6,10</sup>

Based on the results, *IsPET*<sup>MT</sup>, which was expressed and secreted by *E. coli* BL21(DE3), has the potential to be further developed in the future. One of the improvements that can enhance this enzyme is by adding a nonionic surfactant<sup>41</sup> and

anionic surfactants to the low-crystallinity PET film prior to the addition of PETase.<sup>11</sup> Surfactants decrease the hydrophobicity of the polymer surface, facilitating the binding of the enzyme to its substrate. Another improvement that can be used to enhance the binding affinity of this enzyme toward PET substrate is through enzyme fusion with carbohydrate-binding modules, making it easier for the catalytic enzyme to bind with the surface of PET, thus improving PET degradation.<sup>42</sup>

## CONCLUSIONS

To summarize, this study developed an *IsPETase<sup>MT</sup>* that exhibits enhanced thermostability and increased affinity for ligands compared to wild-type *IsPETase<sup>WT</sup>* by combining multiple point mutations. The mutations contribute to a higher affinity for primary ligand 2-HE(MHET)<sub>4</sub> as well as for other polyesters such as 2-HE(MHEF)<sub>4</sub> and MHBT<sub>3</sub>. This strategy has been proven to produce *IsPETase<sup>MT</sup>* with greater degradation of PET plastic film compared to *IsPETase<sup>WT</sup>*. While the degradation activity of *IsPETase<sup>WT</sup>* declines significantly above 40 °C, in contrast, *IsPETase<sup>MT</sup>* maintained high degradation activity up to 60 °C with a melting temperature of 66 °C, which is 15.7 °C higher than that of *IsPETase<sup>WT</sup>*. The quantification of TPA produced after 7 days of incubation using the *IsPETase<sup>MT</sup>* enzyme yielded 0.875 mM TPA. The observed improvements in the *IsPETase<sup>MT</sup>* enzyme highlight its potential for further research and industrial-scale production. Scaling up the production of the PETase enzyme for the industry could pave the way for more sustainable and ecofriendly approaches to managing PET plastic waste.

## ASSOCIATED CONTENT

### Supporting Information

The Supporting Information is available free of charge at <https://pubs.acs.org/doi/10.1021/acsomega.4c05142>.

Detailed mutation prediction on PETase stability

Mutation analysis of PETase; mutation points in the crystal model PETase; SDS-PAGE results of expressed PETase<sup>WT</sup> and PETase<sup>MT</sup>; SDS-PAGE results of purified nontransformed *E. coli* BL21(DE3); and HPLC results of terephthalic acid detection after 7 days of incubation with *IsPETase<sup>MT</sup>* ([PDF](#))

## AUTHOR INFORMATION

### Corresponding Author

**Azzania Fibriani** – School of Life Sciences and Technology, Institut Teknologi Bandung, Bandung 40132, Indonesia; [orcid.org/0000-0003-4319-6966](https://orcid.org/0000-0003-4319-6966); Email: [afibriani@itb.ac.id](mailto:afibriani@itb.ac.id)

### Authors

**Jansen Stevensen** – School of Life Sciences and Technology, Institut Teknologi Bandung, Bandung 40132, Indonesia; [orcid.org/0009-0007-5477-7404](https://orcid.org/0009-0007-5477-7404)

**Rifqi Zahroh Janatunaim** – School of Life Sciences and Technology, Institut Teknologi Bandung, Bandung 40132, Indonesia

**Aisy Humaira Ratnaputri** – School of Life Sciences and Technology, Institut Teknologi Bandung, Bandung 40132, Indonesia

**Safero Hedi Aldafa** – School of Life Sciences and Technology, Institut Teknologi Bandung, Bandung 40132, Indonesia

**Resmila Rachelisa Rudjito** – School of Life Sciences and Technology, Institut Teknologi Bandung, Bandung 40132, Indonesia

**Dwi Hadi Saputro** – Biochemistry and Biomolecular Engineering Research Group, Faculty of Mathematics and Natural Sciences, Institut Teknologi Bandung, Bandung 40132, Indonesia

**Sony Suhandono** – School of Life Sciences and Technology, Institut Teknologi Bandung, Bandung 40132, Indonesia

**Rindia Maharani Putri** – Biochemistry and Biomolecular Engineering Research Group, Faculty of Mathematics and Natural Sciences, Institut Teknologi Bandung, Bandung 40132, Indonesia; [orcid.org/0000-0002-2264-4988](https://orcid.org/0000-0002-2264-4988)

**Reza Aditama** – Biochemistry and Biomolecular Engineering Research Group, Faculty of Mathematics and Natural Sciences, Institut Teknologi Bandung, Bandung 40132, Indonesia; [orcid.org/0009-0006-1797-1059](https://orcid.org/0009-0006-1797-1059)

Complete contact information is available at:  
<https://pubs.acs.org/10.1021/acsomega.4c05142>

### Notes

The authors declare no competing financial interest.

## ACKNOWLEDGMENTS

The authors would like to thank the Faculty of Mathematics and Natural Sciences, Institut Teknologi Bandung for funding this research under contract 100/IT1.C02/SK-TA/2023 and School of Life Sciences and Technology, Institut Teknologi Bandung, for funding this research under Community Improvement and Innovation Program (P2MI) year 2023. We would also like to thank Nicholas Yamahoki who has helped to edit and proofread this manuscript.

## REFERENCES

- (1) Kawai, F. The current state of research on PET hydrolyzing enzymes available for biorecycling. *Catalysts*. **2021**, *11*, 206.
- (2) Statista. ‘Production capacity of polyethylene terephthalate worldwide from 2014 to 2024’. Retrieved from: <https://www.statista.com/statistics/242764/global-polyethylene-terephthalate-production-capacity/>.
- (3) Maurya, A.; Bhattacharya, A.; Khare, S. K. Enzymatic Remediation of Polyethylene Terephthalate (PET)-Based Polymers for Effective Management of Plastic Wastes: An Overview. *Frontiers in Bioengineering and Biotechnology* **2020**, *8*, 1–13.
- (4) Yan, F.; Wei, R.; Cui, Q.; Bornscheuer, U.; Liu, Y. Thermophilic whole-cell degradation of polyethylene terephthalate using engineered Clostridium thermocellum. *Microbial Technology* **2021**, *14* (2), 374.
- (5) Chen, Y.; Zhang, S.; Zhai, Z.; Zhang, M. J.; Liang, X.; Li, Q. Construction of Fusion Protein with Carbohydrate-Binding Module and Leaf-Branch Compost Cutinase to Enhance the Degradation Efficiency of Polyethylene Terephthalate. *Int. J. Mol. Sci.* **2023**, *24* (3), 2780.
- (6) Tournier, V.; Topham, C.; Gilles, A.; David, B.; Folgoas, C.; Moya-Leclair, E.; Kamionka, E.; Desrousseaux, M.; Texier, H.; Gavalda, S.; Cot, M.; Guémard, E.; Dalibey, M.; Nomme, J.; Cioci, G.; Barbe, S.; Chateau, M.; André, I.; Duquesne, S.; Marty, A. An engineered PET depolymerase to break down and recycle plastic bottles. *Nature* **2020**, *580* (7802), 216.
- (7) Yoshida, S.; Hiraga, K.; Taniguchi, I.; Oda, K. Ideonella sakaiensis, PETase, and MHETase: From identification of microbial PET degradation to enzyme characterization. *Methods Enzymol.* **2021**, *648*, 187.
- (8) Son, H. F.; Cho, I. J.; Joo, S.; Seo, H.; Sagong, H. Y.; Choi, S. Y.; Lee, S. Y.; Kim, K. J. Rational Protein Engineering of Thermo-Stable

- PETase from *Ideonella sakaiensis* for Highly Efficient PET Degradation. *ACS Catal.* **2019**, *9*, 3519–3526.
- (9) Sagong, H. Y.; Seo, H.; Kim, T.; Son, H. F.; Joo, S.; Lee, S. H.; Kim, S.; Woo, J. S.; Hwang, S. Y.; Kim, K. J. Decomposition of the PET Film by MHETase Using Exo-PETase Function. *ACS Catalysis*. **2020**, *10*, 4805.
- (10) Oda, M.; Yamagami, Y.; Inaba, S.; Oida, T.; Yamamoto, M.; Kitajima, S.; Kawai, F. Enzymatic hydrolysis of PET: functional roles of three Ca<sup>2+</sup> ions bound to a cutinase-like enzyme, Cut190\*, and its engineering for improved activity. *Appl. Microbiol. Biotechnol.* **2018**, *102*, 10067–10077.
- (11) Furukawa, M.; Kawakami, N.; Tomizawa, A.; Miyamoto, K. Efficient Degradation of Poly(ethylene terephthalate) with Thermo-bifida fusca Cutinase Exhibiting Improved Catalytic Activity Generated using Mutagenesis and Additive-based Approaches. *Sci. Rep.* **2019**, *9*, 1–9.
- (12) Fecker, T.; Galaz-Davison, P.; Engelberger, F.; Narui, Y.; Sotomayor, M.; Parra, L. P.; Ramírez-Sarmiento, C. A. Active Site Flexibility as a Hallmark for Efficient PET Degradation by *I. sakaiensis* PETase. *Biophys. J.* **2018**, *114* (6), 1302–1312.
- (13) Arnal, G.; Anglade, J.; Gavalda, S.; Tournier, V.; Chabot, N.; Bornscheuer, U.; Weber, G.; Marty, A. Assessment of Four Engineered PET Degrading Enzymes Considering Large-Scale Industrial Applications. *ACS Catalysis*. **2023**, *13*, 13156.
- (14) Xu, S.; Huo, C.; Chu, X. Unraveling the Interplay between Stability and Flexibility in the Design of Polyethylene Terephthalate (PET) Hydrolases. *J. Chem. Inf. Model.* **2024**, *64* (19), 7576.
- (15) Schreiber, S.; Gercke, D.; Lenz, F.; Jose, J. Application of an alchemical free energy method for the prediction of thermostable DuraPETase variants. *Appl. Microbiol. Biotechnol.* **2024**, *108* (1), 305.
- (16) Deng, B.; Yue, Y.; Yang, J.; Yang, M.; Xing, Q.; Peng, H.; Wang, F.; Li, M.; Ma, L.; Zhai, C. Improving the activity and thermostability of PETase from *Ideonella sakaiensis* through modulating its post-translational glycan modification. *Commun. Biol.* **2023**, *6* (1), 39.
- (17) Ma, Y.; Yao, M.; Li, B.; Ding, M.; He, B.; Chen, S.; Zhou, X.; Yuan, Y. Enhanced Poly(ethylene terephthalate) Hydrolase Activity by Protein Engineering. *Engineering* **2018**, *4* (6), 888–893.
- (18) Cui, Y.; Chen, Y.; Liu, X.; Dong, S.; Tian, Y.; Qiao, Y.; Mitra, R.; Han, J.; Li, C.; Han, X.; Liu, W.; Chen, Q.; Du, W.; Tang, S.; Xiang, H.; Liu, H.; Wu, B. Computational redesign of a PETase for plastic biodegradation by the GRAPE strategy. *bioRxiv*. **2019**, No. 787069.
- (19) Huang, J.; Rauscher, S.; Nawrocki, G.; Ran, T.; Feig, M.; Groot, B.; Grubmüller, H.; MacKerell. CHARMM36m: an improved force field for folded and intrinsically disordered proteins. *Nat. Methods* **2017**, *14* (1), 71.
- (20) Morris, G. M.; Huey, R.; Lindstrom, W.; Sanner, M. F.; Belew, R. K.; Goodsell, D. S.; Olson, A. J. Autodock4 and AutoDockTools4: automated docking with selective receptor flexibility. *J. Comput. Chem.* **2009**, *16*, 2785–91.
- (21) Trott, O.; Olson, A. J. AutoDock Vina: Improving the speed and accuracy of docking with a new scoring function, efficient optimization, and multithreading. *J. Comput. Chem.* **2009**, *31*, 455.
- (22) Wallace, A. C.; Laskowski, R. A.; Thornton, J. M. LIGPLOT: A program to generate schematic diagrams of protein-ligand interactions. *Protein Eng.* **1995**, *8*, 127–134.
- (23) Pettersen, E. F.; Goddard, T. D.; Huang, C. C.; Couch, G. S.; Greenblatt, D. M.; Meng, E. C.; Ferrin, T. E. UCSF Chimera - A Visualization System for Exploratory Research and Analysis. *J. Comput. Chem.* **2004**, *25* (13), 1605–1612.
- (24) SYSTÈMES, D. BIOVIA Discovery Studio Dassault Syst. mes BIOVIA, *Discovery Studio Modeling Environment*, 2016 Release 2017. Dassault Systems.
- (25) Yang, H.; Wong, M. W. Oxyanion hole stabilization by C-H-O Interaction in a transition state - a three-point interaction model for cinchona alkaloid-catalyzed asymmetric methanolysis of meso -cyclic anhydrides. *J. Am. Chem. Soc.* **2013**, *135*, 5808–5818.
- (26) Shi, L.; Liu, H.; Gao, S.; Weng, Y.; Zhu, L. Enhanced extracellular production of *Is*PETase in *Escherichia coli* via Engineering of the pelB signal peptide. *Agric. Food Chem.* **2012**, *60* (7), 2245.
- (27) Grote, A.; Hiller, K.; Scheer, M.; Munch, R.; Nortemann, B.; Hempel, D. C.; Jahn, D. JCat: a novel tool to adapt codon usage of a target gene to its potential expression host. *Nucleic acids research* **2005**, *33* (Web Server issue), W526–W531.
- (28) Son, H. F.; Joo, S.; Seo, H.; Sagong, H. Y.; Lee, S. H.; Hong, H.; Kim, K. J. Structural bioinformatics-based protein engineering of thermo-stable PETase from *Ideonella sakaiensis*. *Enzyme Microb. Technol.* **2020**, *141*, No. 109656.
- (29) Joo, S.; Cho, I. J.; Seo, H.; Son, H. F.; Sagong, H. Y.; Shin, T. J.; Choi, S. Y.; Lee, S. Y.; Kim, K. J. Structural insight into molecular mechanism of poly(ethylene terephthalate) degradation. *Nat. Commun.* **2018**, *9* (1), 382.
- (30) Han, X.; Liu, W.; Huang, J. W.; Ma, J.; Zheng, Y.; Ko, T. P.; Xu, L.; Cheng, Y. S.; Chen, C. C.; Guo, R. T. Structural insight into catalytic mechanism of PET hydrolase. *Nat. Commun.* **2017**, *8* (1), 2106.
- (31) Liu, C.; Shi, C.; Zhu, S.; Wei, R.; Yin, C. C. Structural and functional characterization of polyethylene terephthalate hydrolase from *Ideonella sakaiensis*. *Biochem. Biophys. Res. Commun.* **2019**, *508* (1), 289–294.
- (32) Kumar, S.; Tsai, C. J.; Nussinov, R. Factors enhancing protein thermostability. *Protein engineering* **2000**, *13* (3), 179–191.
- (33) Brott, S.; Pfaff, L.; Schuricht, J.; Schwarz, J.; Böttcher, D.; Badenhorst, C.; Wei, R.; Bornscheuer. Engineering and evaluation of thermostable Is PETase variants for PET degradation. *Eng. Life Sci.* **2022**, *22* (3–4), 192–203.
- (34) Shroff, R.; Acosta, D.; Alexander, B.; Cole, H.; Zhang, Y.; Lynd, N.; Ellington, A.; Alper, H.; Lu, H.; Diaz, D.; Czarnecki, N.; Zhu, C.; Wantae, Kim Machine learning-aided engineering of hydrolases for PET depolymerization. *Nature* **2022**, *604*, 662.
- (35) Yoshida, S.; Hiraga, K.; Takehana, T.; Taniguchi, I.; Yamaji, H.; Maeda, Y.; Toyohara, K.; Miyamoto, K.; Kimura, Y.; Oda, K. A bacterium that degrades and assimilates poly(ethylene terephthalate). *Science* **2016**, *351*, 1–5.
- (36) Bell, E. L.; Smithson, R.; Kilbride, S.; Foster, J.; Hardy, F. J.; Ramachandran, S.; Tedstone, A. A.; Haigh, S. J.; Garforth, A. A.; Day, P. J. R.; Levy, C.; Shaver, M. P.; Green, A. P. Directed evolution of an efficient and thermostable PET depolymerase. *Nature Catalysis* **2022**, *5*, 673–681.
- (37) Austin, H.; Allen, M.; Donohoe, B. Characterization and engineering of a plastic-degrading aromatic polyesterase. *Proc. Natl. Acad. Sci. U.S.A.* **2018**, *115* (19), No. E4350.
- (38) Menzel, T.; Weigert, S.; Gagsteiger, A.; Eich, Y.; Sittle, S.; Papastavrou, G.; Ruckdäschel, H.; Altstädt, V.; Höcker, B. Impact of enzymatic degradation on the material properties of poly(ethylene terephthalate). *Polymers* **2021**, *13* (22), 3885.
- (39) Thomas, C.; Geer, D. Effects of shear on proteins in solution. *Biotechnol. Lett.* **2011**, *33* (3), 443.
- (40) Wei, R.; Song, C.; Gräsing, D.; Schneider, T.; Bielytskyi, P.; Böttcher, D.; Matysik, J.; Bornscheuer, U. T.; Zimmermann, W. Conformational fitting of a flexible oligomeric substrate does not explain the enzymatic PET degradation. *Nat. Commun.* **2019**, *10*, 5581.
- (41) Caparanga, A.; Basilia, B.; Dagbay, K.; Salvacion, J. Factors affecting degradation of polyethylene terephthalate (PET) during pre-flotation conditioning. *Waste Management* **2009**, *29* (9), 2425.
- (42) Wang, T.; Yang, W.; Gong, Y.; Zhang, Y.; Fan, X.; Wang, G.; Lu, Z.; Liu, F.; Liu, X.; Zhu, Y. Molecular engineering of PETase for efficient PET biodegradation. *Ecotoxicol. Environ. Saf.* **2024**, *280*, No. 116540.